Dynamical NL Optics, Bistability

Dynamic Nonlinear Optics in Semiconductors

A. Miller

Royal Signals and Radar Establishment, St. Andrews Road, Malvern, Worcs WR 14 3PS, UK

D. A. B. Miller

Bell Laboratories, Holmdel, NJ 07733, USA

PACS: 42.65

Semiconducting materials have for some time been of interest for non-linear optical applications such as harmonic generation and parametric amplification and more recently for optical bistable and associated devices. In general, *passive* optical nonlinearities in semiconductors arising from the interaction of *intense* laser radiation fields with bound valence electrons (normally through the second order susceptibility coefficient, $\chi^{(2)}$) are relatively large. In the past few years, *active* nonlinear processes in semiconductors have attracted considerable attention whereby charge carrier redistribution takes place among the energy bands due to the optical excitation. It has been found that a relatively small number of excited carriers can have profound effects on the optical properties which will be significant for optical signal processing applications if a suitable combination of nonlinearity and fast time response can be achieved compatible with optical communications system. This summary can only briefly review our present understanding of the electron dynamics associated with active optical nonlinearities in semiconductors and offer a few examples. For a fuller account, see the recent review by Miller et al. [1].

Both absorptive and refractive properties of semiconductors are modified by carrier redistribution and can often be formulated in terms of the real and imaginary parts of the third order susceptibility,

$$P_i^{\omega_4} = \chi_{ijkl}^{(3)} E_j^{\omega_1} E_k^{\omega_2} E_l^{\omega_3}.$$

Measured values of $\chi^{(3)}$ range between 10^{-11} e.s.u. for GaAs away from resonance to 1.0 e.s.u. in InSb at near-resonance to the band gap energy at 77 K. This enormous difference from the passive non-resonant situation is explained by *band-gap resonant saturation* effects [2] which can be induced by relatively weak laser fields.

For the strong direct optical transitions between bands, the states coupled optically are effectively those of the same k-value since photon momentum can be considered negligible. The energy separation varies from k-value to k-value and so the system appears similar to an *inhomogeneous* atomic absorber although it should be remembered that for a solid, the states involved are extended states throughout the whole crystal. If there is no transfer of excitation between the various optically coupled states, the semiconductor will behave like an inhomogeneous atomic system. In this case, called *state-filling*, the relaxation takes place either directly between the optically coupled states or through other non-saturating states not involved in the absorption. For instance, in the saturation of intervalence band absorption in p-type semiconductors, relaxation is via fast optical phonon scattering which removes the carriers entirely from states involved in the optical interaction [3, 4]. In general, scattering times in semiconductors (and hence the dephasing time, T_2) are short, $10^{-12}-10^{-14}$ s, with the result that high intensities are needed to induce state-filling saturation and coherent phenomena are difficult to observe. Scattering may be dominated in different cases by phonons, ionized impurity centres or carrier-carrier interactions [5].

Absorption saturation can also occur when the transfer of excited carriers between states results in the progressive filling of an energy band, i.e. *band-filling* saturation, sometimes called dynamic Burstein-Moss shifting. The created carrier populations are scattered rapidly through Coulomb interactions usually towards quasi-equilibrium thermal distributions to give some effective temperature for both electrons and holes which is different from that of the lattice since the carriers are excited to some excess energy above the band extremum [6]. Subsequent cooling of these Fermi-like distributions take place predominantly through the emission of longitudinal optical phonons generally in a few picoseconds although screening of the electron-phonon interaction at high densities [7] and bottlenecking of the optical phonon de-excitation [8] may increase this relaxation time. Finally the excited carriers recombine on timescales which can be as long as hundreds of microseconds or shorter than a nanosecond depending on the conditions. To complete the picture of the electron dynamics after excitation, the diffusion of the carriers must be considered. The initial spatial distribution of optically generated carriers through a crystal will be inhomogeneous unless the thickness is much less than an absorption length. The transverse spatial distribution is also important for such effects as self-focusing and also when the optical parameters are spatially modulated by the interference of two beams coincident in time and space in the sample. Carrier diffusion can rapidly wash out these inhomogeneities before the carriers recombine.

In the absence of detectors and electronics with sufficiently fast response times, studies of optically induced electron dynamics on a picosecond timescale have been carried out using the excite-probe technique with mode-locked lasers. A variable spatial delay in the excite beam path provides the picosecond timescale. For instance, saturation in germanium has been studied extensively at 1.06 μm using Nd:glass lasers [6]. Although germanium has an indirect gap, this wavelength allows direct excitation near the zone centre with a large excess energy. An apparent slow cooling of the carrier distribution taking several hundred picoseconds has been observed and analysed [9] and at the highest excitation levels, an induced absorption due to transitions from the spin-orbit split band to the upper valence levels limits the optical transmission [10]. The band gap energy of GaAs is accessible with dye lasers and has shown a wealth of nonlinear transmission effects. High power, subpicosecond pulses with a wavelength continuous probe pulse have been used to study the dynamics of band filling and cooling, band gap renormalisation and the screening of the free exciton absorption line at optically generated high carrier densities [11]. The carrier dynamics in microstructure layers sufficiently thin that quantum effects become important have been analysed [12] and recently hot electron velocity overshoot measured in GaAs on a picosecond timescale [13].

Significantly for device applications, very strong nonlinearities have been observed with low power cw lasers. The saturation intensity of the excitonic resonance in a thin layer of GaAs at 10 K has been measured at 150 W/cm^2 [14]. The associated refractive index changes have resulted in successful demonstration of fast (<1 ns) optical bistable switching [15]. Absorption in low band gap materials such as InSb can be saturated for photon energies in excess of the band gap energy with 100 W/cm^2 [16]. For photon energies below the band gap, residual absorption shows strong saturation effects but the physical mechanisms are still a subject for further study [17]. Also in this region, very strong nonlinear refraction due to blocking of interband transitions by generated carriers [2] has led to optical bistability at power levels as low as 8 mW [18]. Both InSb [19] and $Cd_xHg_{1-x}Te$ [20] allow degenerate four wave mixing at cw powers for photon energies close to the band gap energy.

These and other studies not mentioned here are now producing a wealth of new information on the dynamics of optically induced electronic processes in semiconductors and may well lead to the realisation of fast all-optical processing devices for use with low power lasers.

1. A. Miller, D. A. B. Miller, S. D. Smith: Adv. Phys. (1981)
2. D. A. B. Miller, C. T. Seaton, M. E. Prise, S. D. Smith: Phys. Rev. Lett. **47**, 197 (1981)
3. F. Keilman: IEEE J. QE-**12**, 592 (1976)
4. R. B. James, D. L. Smith: Phys. Rev. B **21**, 3502 (1980)
5. R. G. Ulbrich: Solid State Electr. **21**, 51 (1978)
6. A. Elci, M. O. Scully, A. L. Smirl, J. C. Matter: Phys. Rev. B **16**, 191 (1977)
7. E. J. Yoffa: Phys. Rev. B **23**, 1909 (1981)
8. H. M. Van Driel: Phys. Rev. B **19**, 5928 (1979)
9. A. L. Smirl, A. Miller, G. P. Perryman, T. Boggess: Proc. 3rd Int. Conf. Hot Carriers in Semiconductors (Montpellier, July 1981)
10. A. Miller, G. P. Perryman, A. L. Smirl: Opt. Commun. **38**, 289 (1981)
11. C. V. Shank, R. L. Fork, R. F. Leheny, J. Shah: Phys. Rev. Lett. **42**, 112 (1979)
12. R. L. Fork, C. V. Shank, B. I. Greene, R. K. Reinhart, R. A. Logan: *Picosecond Phenomena II*, Springer Series in Chemical Physics, Vol. 14, ed. by R. Hochstrasser, W. Kaiser, C. V. Shank, (Springer, Berlin, Heidelberg, New York 1981) p. 280
13. C. V. Shank, R. L. Fork, B. I. Greene, F. K. Reinhart, R. A. Logan: Appl. Phys. Lett. **38**, 104 (1981)
14. H. M. Gibbs, S. L. McCall, A. Passner, W. Weigmann, T. N. C. Venkatesan: Solid State Commun. **30**, 271 (1979)
15. H. M. Gibbs, S. L. McCall, T. N. C. Venkatesan, A. C. Gossard, A. Passner, W. Wiegmann: Appl. Phys. Lett. **35**, 451 (1979)
16. P. Lavallard, R. Richard, C. Benoit a la Guillaume: Phys. Rev. B **16**, 2804 (1977)
17. D. A. B. Miller: Proc. Royal Soc. (in press)
18. D. A. B. Miller, S. D. Smith, C. T. Seaton: IEEE J. QE-**17**, 312 (1981)
19. D. A. B. Miller, R. G. Harrison, A. M. Johnston, C. T. Seaton, S. D. Smith: Opt. Commun. **32**, 478 (1980)
20. M. A. Khan, R. L. H. Bennet, P. W. Kruse: Opt. Lett. **6**, 560 (1981)

Photoemission Yield Under Multiple Quantum Excitation

M. Bensoussan and J. M. Moison

Centre National d'Etudes des Télécommunications, PAB/PMS/OMT, F-92220 Bagneux, France

PACS: 42.65

Multiquantum photoemission (MQP) is a non linear photoelectric effect in which several quanta are simultaneously absorbed in electronic transitions rising electrons up to the vacuum level. Conservation of energy require that the sum of the absorbed energies be equal or greater than the work function. MQP has much in common with nonlinear optics but has the added complication that the excited electron must escape from the solid before it is observed. This effect makes the interpretation more difficult but as we shall see it may be used as an advantage in the study of the electronic structure of a solid. Like all the fields of nonlinear optics the studies of MQP takes advantage of the latest progresses made in laser sources. The quality of the experimental data is highly related to that of the laser used and of the characteristics of the beam features. Conclusive experiments aimed to establish the existence of MQP especially for high order are scarce.

A fairly detailed review of the investigation carried out on MQP until 1977 can be found in [1]. Here we concentrate our attention on the more recent results and five specific problems are covered: (1) the experimental limitations to the observation of MQP, (2) the trends of the quantum yield as a function of material and process-order, (3) the two quantum photoemission yield spectra, (4) the surface contribution to MQP, (5) the phenomenological model accounting for the two quantum photoemission in silicon.

Because of the consequences of the experimental conditions on the observation of MQP it is necessary to define the working range as a function of the detection limit, the space charge effects and the thermal effects. The last ones are the most interfering effects since high photon fluxes are usually necessary to get a detectable non linear photoemission signal. It is well accepted now that at laser intensities higher than some threshold value, heating of the surface of the sample occurs. Moreover, we have established in silicon [2] that before any modification of the surface, such as vaporization melting or even reconstruction, becomes apparent, the rise in temperature leads to the well-known thermoemission or thermally assisted MQP processes. At moderate temperatures thermally MQP prevails, mostly near the apparent photoelectric threshold and the higher the order the more cumbersome it is. At sufficiently high temperature thermoemission described by the classical Richardson's law is the outstanding effect and completely obscures photoemission. Very recently because of its intimate relation with laser annealing, pulsed laser heating has suddenly become a blooming field. A large number of theoretical and experimental papers are available in this field. Even so it seems that no comprehensive understanding of the underlying mechanisms is reached and consequently no simple criterion for the estimate of the surface temperature rise under laser irradiation has become clear. Let us note that nonlinear photoemission is indeed among the best tools to determine the surface temperature during the laser pulse and then as we are especially concerned by MQP, heating can be strictly avoided.

The fluxes relation $J_e = Y_n J_{ph}^n$ defines the n-order multiquantum yield Y_n which in turn completely describe the phenomenon. J_e and J_{ph} are respectively electron and photon fluxes. MQP with n as high as 8 has been reported, but no quantitative measurements for such higher order are available. Moreover even when $n \leqq 4$ for which quantitative results exist it is not always very easy to deduce precise absolute values of Y_n. The reasons for that will be discussed, we, nevertheless present in the following table some values of Y_n whose main interest is to give the trends as a function

of materials and order. The correlation of these trends with the underlying mechanisms will be tentatively approached.

Materials	Y_2 [cm^2 s]	Y_3 [cm^4 s^2]	Y_4 [cm^6 s^3]
Metals and semiconductors	$10^{-37}-10^{-33}$	10^{-62}	$10^{-96}-10^{-92}$
Alkali antimonides	$10^{-31}-10^{-29}$	10^{-56}	
Organic crystals	$10^{-27}-10^{-25}$		

The dependence of the MQP photocurrent on the photon energy is of considerable interest and must give more insight into the underlying processes. To our knowledge only a few studies have been reported because of considerable technical difficulties among which, for n higher than 2, the lack of tunable wavelength picosecond lasers. The only one is on anthracene [3] where the two quantum yield is so high that a conventional light source could be used. The two other cases, PbI_2 and GaS on one hand [4] and Si on the other [5], are more recent and were performed with a dye laser pumped by a nitrogen laser as light source. The differences and the similarities between these three cases will be analysed. We may lay some emphasis on the additional new information that two quantum yield spectrum brings about the intermediate levels.

An old controversy has dealt with the ratio of surface and volume contributions to MQP and the question of their separation. The classical method of doing it is to take advantage of the vectorial effects by studying the yield as a function of incident angle and polarization. Indeed an enhancement of photocurrent with varying the angle of incidence and with peaking at a given angle has been reported on Au for $n=5$ [6] and on W for $n=2$ and $n=4$ [7]. For Au the MQP is a pure surface effect while for W both surface and volume contribute to the MQP. These interpretations are based however on the a priori assumption that volume excitation is isotropic and that volume and surface contributions are simply additive. Because of the finite escape depth the photoemitted spectrum may contain significant contributions from the surface region where the density of state differs from that in the bulk. We have performed the first experiment pertaining to surface specific properties of clean surface on Si which possesses occupied surface states in the band gap [8]. These surface states are induced by dangling bonds. At photon energy equal to 2.64 eV the only possible initial state for any emitted electron in a two quantum photoemission lies in the surface state band. It is well established that this bond is removed by oxygen adsorption which does not create any other effect. After such processing we accordingly observe that the photoemission yield falls below our experimental limit. These results may open a new field of research in surface effects contributions to MQP.

To date theoretical estimates of MQP yields do not seem to be sufficiently reliable to provide the basis for a quantitative discussion. Accordingly we propose a phenomenological approach which consists in extending to the MQP the three steps model which is remarkably successful in the interpretation of the one quantum photoemission. In fact we shall consider only the two quantum photoemission case and apply the model to Si where a maximum of data are available. The model is presented with the emphasis put on the multiple excitation which brings electrons up the vacuum level while photon energy is less than the work function. The two elementary processes put forward to interpret the results are nonlinear optical absorption (two photon absorption) and non radiative Auger recombination (bimolecular process). Both processes give a good order of magnitude of the observed yields and hence it is possible that both be actually operative and produce overlapping spectra.

In conclusion MQP studies are still in their infancy if one compares to the effort developed in linear photoemission field for example, and enough important questions remain open to stimulate further work. Two photon photoemission is a promissing spectroscopy tool for studying empty states between Fermi level and vacuum, and hot electron effects. Finally the reasonable extension to the use of the two beams would be briefly outlined.

1. S.J. Anisimov, V.A. Benderskii, G. Farkas: Sov. Phys. Usp. **20**, 467 (1977)
2. M. Bensoussan, J.M. Moison: J. Phys. (Paris) (in press, 1982)
3. G.T. Pott, D.F. Williams: J. Chem. Phys. **51**, 203 (1969)
4. A. Kasuya, Y. Nishina: J. Phys. Soc. Jpn. **50**, 97 (1981)
5. J.M. Moison, M. Bensoussan: Solid State Commun. **39**, 1213 (1981)
6. L.A. Lompre, J. Thebault, G. Farkas: Appl. Phys. Lett. **27**, 110 (1975)
7. R. Yen, P. Liu, M. Dagenais, N. Bloembergen: Opt. Commun. **31**, 334 (1979)
8. M. Bensoussan, J.M. Moison, B. Stoesz, C. Sébenne: Proceeding of the Fourth J.C.S.S. and of the third ECSS Cannes (1980) p. 1197

Degenerate Four-Wave Mixing at the Band Edge of InAs

D. C. Haueisen

Pacific Lutheran University and Air Force Weapons Laboratory, Albuquerque, NM 87117, USA

D. A. Depatie

Air Force Weapons Laboratory, Albuquerque, NM 87117, USA

PACS: 42.65

There has been considerable recent attention given to degenerate four-wave mixing (DFWM) in semiconductors near the band edge where the third order susceptibility can become large and high mixing efficiences achieved [1–3]. We report experimental data and theoretical calculations for the frequency and intensity dependence of forward DFWM in n-type InAs.

Measurements have been made with a room temperature sample of 0.15 mm thickness using a line tunable, pulsed DF laser. The wavelength varied from 3.6 μm to 4.0 μm, extending across the band edge with the absorption constant ranging from 2 cm^{-1} to 200 cm^{-1}. The efficiency of DFWM as a function of frequency is first increasing as the band edge is approached from below, due to an increase in the nonlinear susceptibility, and then decreasing as linear absorption dominates. As a function of pump intensity, the expected dependence of efficiency on the second power of pump intensity is observed only for the longer wavelengths and pump intensity on the order of 10 kW/cm^2. Saturation of the efficiency occurs for higher pump intensity and more severe saturation as the band edge is approached. The maximum DFWM efficiency measured was 30% for a pump intensity on the order of 1 MW/cm^2 and for the sample thickness about equal to the absorption length.

The theoretical model used to describe the nonlinear susceptibility is that of an induced index grating [4] in the semiconductor produced by the interference of the pump and probe beams. This intensity dependent free carrier density grating diffracts the

original pump field to produce the signal. For low pump power, an analytical expression for the mixing efficiency has been obtained under the assumption that pump depletion and the optical Kerr effect can be ignored, but including attenuation of all beams. The agreement between theory and experiment in this region is good. The only adjustable parameter in the calculation is the grating decay time, dominated by electron-hole recombination in these experiments, for which the value of 10^{-8} s is obtained. For higher pump power, the mixing equations have been solved numerically including absorption, pump depletion and the optical Kerr effect. Results predict saturation in substantial agreement with the measurements. Calculated values of the nonlinear susceptibility in these experiments were as large as 5×10^{-4} e.s.u.

1. R.K.Jain, M.B.Klein, R.C.Lind: Opt. Lett. **4**, 328 (1979)
2. D.A.B.Miller, R.G.Harrison, A.M.Johnston, C.T.Seaton, S.D.Smith: Opt. Commun. **32**, 478 (1980)
3. A.L.Smirl, T.F.Boggess, F.A.Hopf: Opt. Commun. **34**, 463 (1981)
4. R.K.Jain, M.B.Klein: Appl. Phys. Lett. **35**, 454 (1979)

Mechanisms of Optical Phase Conjugation in $Hg_{1-x}Cd_xTe$

P. W. Kruse and M. A. Khan
Honeywell Corporate Technology Center, Bloomington, MN 55420, USA

PACS: 42.65

$Hg_{1-x}Cd_xTe$ is an alloy semiconductor which is in widespread use for infrared radiation detection. The forbidden energy gap is dependent upon composition (x-value) and temperature. Compositions with $x \sim 0.2$ have en energy gap of ~ 0.1 eV at 77 K. The electron effective mass in this composition range is ~ 0.01 and the conduction band is nonparabolic. Thus the spin-level splitting factor (g-value) is large, e.g., 80 for $x = 0.23$, and strongly dependent upon composition.

For these reasons, $Hg_{1-x}Cd_xTe$ is an excellent material for nonlinear optical studies, especially near 10 μm wavelength. These include optical phase conjugation in samples pumped by means of a CO_2 laser. We have investigated optical phase conjugation by four-wave mixing in $Hg_{1-x}Cd_xTe$ in the composition range $x = 0.21$–0.23. Three experiments, depending upon three mechanisms, have been carried out. These include spin-resonant nondegenerate four-wave mixing, nonresonant degenerate four-wave mixing, and bandgap-resonant degenerate four-wave mixing.

Spin-resonant nondegenerate four-wave mixing experiments [1] are carried out at 4 K using two CO_2 lasers operating at different optical frequencies. A magnetic field in which the sample is immersed is adjusted so that the conduction band spin-level splitting energy equals the energy difference between the pump lasers. We find a third order susceptibility of 1×10^{-4} e.s.u, a phase conjugation power reflection coefficient of up to 1%, and a pumping threshold of about 10–10^2 W cm^{-2}.

Nonresonant degenerate four-wave mixing experiments [2] are carried out at 4 K, 77 K, and 295 K. A CO_2 TEA laser is the source of pump and probe beams. The energy of the CO_2 laser is insufficient to excite hole-electron pairs. Under these conditions conduction band nonparabolicity is responsible for the third order nonlinearity. We find the third order susceptibility to be in the 10^{-8}–10^{-7} e.s.u. range, the phase conjugate power reflection coefficient to be up to 8%, and the pumping threshold to be 10^4–10^5 W cm^{-2}.

Bandgap resonant degenerate four-wave mixing experiments [3] are carried out at the temperature at which the energy gap is coincident with the energy of the Q-switched CO_2 laser employed for the pump and probe beams. For the $x = 0.216$ composition this occurs at 60–70 K. In this case we find the third order susceptibility to be as high as 3×10^{-2} e.s.u., the phase conjugate power reflection coefficient to be up to 10%, and the pumping threshold to be as low as 10^{-1} W cm^{-2}.

Miller et al. [4] have discussed the mechanisms which may be operable in InSb phase conjugation under bandgap resonant conditions at 5 μm. They find that interband saturation-induced nonlinear refraction to be the most plausible mechanism. We shall discuss our bandgap-resonant four-wave mixing results in terms of the several mechanisms discussed by Miller, including the photoexcited free hole-electron plasma model of Jain and Klein [5].

1. P.W.Kruse, M.A.Khan, J.F.Ready: Optical Phase Conjugation in (Hg, Cd)Te, SPIE 25th Annual International Technical Symposium and Exhibit, San Diego, August 24–28, 1981
2. M.A.Khan, P.W.Kruse, J.F.Ready: Opt. Lett. **5**, 261 (1980)
3. M.A.Khan, R.L.H.Bennet, P.W.Kruse: Opt. Lett. **6**, 560 (1981)
4. D.A.B.Miller, S.D.Smith, B.S.Wherrett: Opt. Commun. **35**, 221 (1980)
5. R.K.Jain, M.B.Klein: Appl. Phys. Lett. **35**, 454 (1979)

Degenerate Four-Wave Mixing by Anisotropic State-Filling in Semiconductors

A. L. Smirl, B. S. Wherrett, T. F. Boggess, G. P. Perryman, and A. Miller
Center for Applied Quantum Electronics, North Texas State University Denton, TX 76203, USA

PACS: 42.65

New experimental and theoretical results are presented for degenerate four-wave mixing under conditions of intense picosecond laser irradiation in excite-probe experiments. We distinguish between two transient-grating sources for the mixing: the concentration grating that has been discussed previously and an additional, *orientational grating*. Our experimental results for germanium involve a feature that is consistent only with the presence of an orientational grating. This leads us to conclude that we have established *anisotropic state-filling* in this semiconductor, the first direct observation of such an effect. Further we derive different symmetry characteristics for self-diffraction from the two types of gratings and show how their investigation may be used to measure k-state diffusion (momentum relaxation) rates in semiconductors or molecular reorientation rates in liquids.

In our experiments single 1.06 μm, 7 ps pulses produced by a mode-locked Nd:glass laser were divided by a beam splitter and a variable delay introduced into one path. The delayed (probe) pulse was attenuated by a factor greater than 10^3 and the two pulses recombined at a small angle (θ) on the surface of a 5.7 μm thick wafer of crystalline germanium. The probe transmission was measured as a function of time delay (Fig. 1). Inspection of Fig. 1a

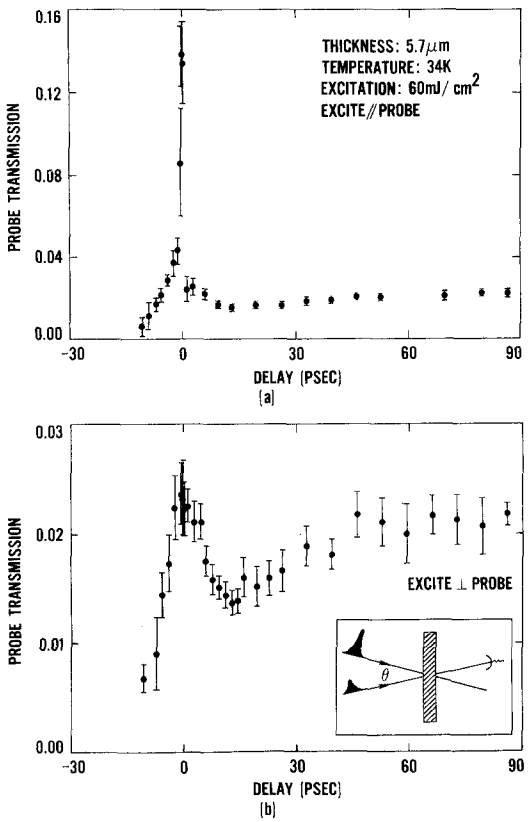

Fig. 1a and b. Probe transmission as a function of time delay between the excite and probe pulses for the polarization of the electric field of the probe pulse arranged (a) parallel and (b) perpendicular to that of the exciting pulse

reveals three distinct features. The most prominent is a rapid rise and fall in probe transmission (~2 ps, FWHM) centered about zero delay. This "correlation spike" has been interpreted previously as the self-diffraction of the excite beam into the probe direction. Modulation of the spatial concentration of excited carriers whilst the two beams overlap spatially and temporally will produce such a spike. Over a period of hundred of picoseconds, there is a gradual rise and fall that has also been studied previously and is not the subject of investigation here.

Careful examination of the structure near zero delay reveals that the narrow spike is superposed on a broader peak, approximately 10 ps wide. This feature, which has not been observed previously, can be shown to be distinct from the narrower correlation spike by repeating the experiments with the probe polarization rotated perpendicular to that of the excite pulse (Fig. 1b) – in the experiments of Fig. 1a the polarizations were parallel. Only the broader peak remains for the orthogonal configuration; the sharp correlation spike is absent. Further measurements in the background-free $(-\theta)$ direction confirm this polarization dependence. Note that the self-diffracted wave at $-\theta$ is also the forward-traveling phase-conjugate wave and that anisotropic state-filling is a new mechanism contributing to the degenerate four-wave mixing process.

The polarization characteristics of the broader spike are consistent only with the presence of an orientational grating. By such a grating we mean that there is a preferential orientation (in k-space) of the optically excited states. The broad feature is indeed observed only at the highest excitation levels ($\sim 10^{10}\,\mathrm{W\,cm^{-2}}$), where the carrier generation rate into energy states in any given k-direction might be expected to become comparable to the momentum relaxation rate out of these states. The point is that an orientational grating can exist even for the orthogonal polarization configuration, a configuration for which the laser irradiance is uniform in space and there is no modulation of the concentration of excited carriers – no concentration grating. The orientational grating is still present because the k-direction of the predominant orientation of the excited states will be modulated in real space. (In the parallel configuration the intensity and hence the concentration of excited states varies spatially but the preferred orientation is fixed.)

We show theoretically that if the preferential orientation is strictly maintained then the *symmetry* associated with the self-diffraction is that of the third-order nonlinear susceptibility $\chi^{(3)}_{ijkl}$, for both polarization configurations. For the perpendicular configuration, this is the symmetry of the entire self-diffraction. However, for parallel polarizations that portion of the grating which still remains after reorientation leads to self-diffraction of symmetry $\chi^{(1)}_{ij}\chi^{(1)}_{kl}$. In general both symmetry types will be present for the parallel configuration. We discuss the different tensor natures for our germanium model and for a molecular model.

Having established that the orientational and concentration gratings can be distinguished experimentally, we note also that a concentration grating will decay partially by angular reorientation but can be completely destroyed only by deexcitation or spatial diffusion. In contrast all three mechanisms can eliminate purely orientational gratings. Hence the study of these sources of self-diffraction can be used to measure the momentum relaxation rate in solids (or molecular reorientation times in liquids).

Room-Temperature Saturation Characteristics of GaAs–GaAlAs Multiple Quantum Well Structures and of Bulk GaAs

D. A. B. Miller, D. S. Chemla, and P. W. Smith
Bell Laboratories, Holmdel, NJ 07733, USA
A. C. Gossard and W. T. Tsang
Bell Laboratories, Murray Hill, NJ 07974, USA

PACS: 42.65

In this paper we report the first observation of saturation of the exciton absorption in GaAs:GaAlAs multiple quantum well (MQW) structures at 300 K. We study the comparison of this saturation with that seen in GaAs in which we also resolve the excitonic saturation contribution at 300 K.

Previous studies of the optical properties of GaAs:GaAlAs multiple quantum well (MQW) heterostructure material have concentrated on low-temperature behavior [1, 2] as have previous observations of GaAs exciton saturation [3]. Our studies have disclosed some new features which are of interest for an understanding of the physics of these structures, and are important for potential device applications.

In Fig. 1 we show the low intensity *room temperature* absorption spectra of, respectively, a 3.2 μm thick undoped GaAs sample and a 2.11 μm thick MQW sample. The latter consists of alternate 145 Å GaAs layers and 196 Å $Ga_{0.72}Al_{0.28}As$ layers. These spectra are taken with a conventional spectrometer system of

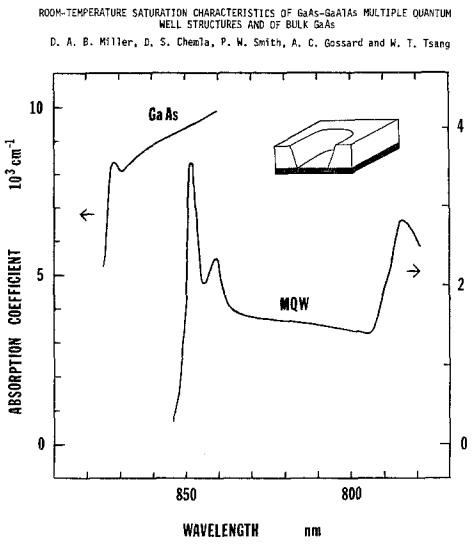

Fig. 1. Room temperature absorption spectra of a 3.2 μm GaAs sample and a 2.11 μm GaAs:GaAlAs MQW superlattice sample. Both samples are grown by molecular beam epitaxy on GaAs substrates. The substrate is etched away to leave the epitaxial layers exposed over $a \sim 1\,mm^2$ area, as shown in cross section in the inset above. The GaAs sample is sandwiched between two transparent GaAlAs layers also of 3.2 μm thickness. The absorption scale for GaAs also applies to the MQW structure if only the total GaAs thickness (0.90 μm) in the MQW is used in calculations

resolution $\lesssim 3$ Å and are corrected for surface reflections. In the GaAs spectrum the exciton peak is just distinguishable; in contrast both the light and heavy exciton peaks of the MQW sample are well resolved at room temperature. This very attractive feature results from the 2-dimensional (2D) nature of the electron-hole gas in MQW structures, which increases the exciton binding energy and modifies their dissociation by phonons.

Saturation of absorption of both samples at the exciton energy and above has been studied at 300 K using a cw oxazine 750 infrared dye laser pumped by a Krypton ion laser. The saturation intensity of MQW excitons is approximately three times smaller than that of the bulk GaAs and of the order of $1\,kW/cm^2$. Experimental and theoretical work is in progress to compare saturation effects in 2D and 3D systems.

The fact that sharp and easily-saturable excitonic features can be found at room temperature in properly-designed MQW structures has important implications for device applications. The large refractive index changes associated with the saturation of the exciton peak should permit the fabrication of compact, monolithic, integrated optical switches and control elements directly compatible with semiconductor laser and integrated waveguide structures.

1. See, for example C. Weisbuch et al.: Inst. Phys. Conf. Ser. No. 56, Inst. of Physics (London) (1981) p. 711
2. C. V. Shank, R. L. Fork, B. I. Greene, C. Weisbuch, A. C. Gossard: Surf. Sci. (in press, 1982)
3. H. M. Gibbs et al.: Solid State Commun. **30**, 271 (1979)

Observation of a Mott Transition in GaP:N

S. Chu, P. Hu, and T. M. Jedju
Bell Laboratories, Murray Hill, NJ 07974, USA

PACS: 42.65

As the density of excitons is increased to the point where their average separation is a few exciton Bohr radii, they are expected to undergo a Mott transition [1]. This transition, which is sudden at $T = 0$ K, can be thought of as the screening of the electron-hole attraction by other electron-hole pairs to the point where the electrons and holes are no longer bound to each other.

In previous studies of exciton systems where standard fluorescence techniques were used to monitor the behavior of the excitons, one sees spectra indicating both excitons in a low density state and an electron-hole liquid or plasma in a high density state roughly an order of magnitude higher density than the Mott value. Although the appearance of a high density electron-hole state indicates that a screening process does occur, it is difficult to establish via fluorescence that a true Mott transition occurs. For example, in germanium, the free excitons created at an average density far below the Mott density can still form an electron-hole liquid [2]. Even when the excitons are nominally bound to impurity sites, as in the case of GaP:N, the appearance of a plasma or liquid-like structure does not appear suddenly as the exciton density is increased [3].

In our experiment, we excite the $J = 1$ exciton pinned to a nitrogen impurity site. We use a picosecond dye laser to write a standing wave of excitation with two laser beams, and measure the decay of the grating with a third beam. By comparing long and short periodicity gratings, we find that below a critical exciton density, the excitons decay to a $J = 2$ state 0.8 meV below the $J = 1$ state in roughyl 300 ps, and then slowly diffuse with characteristic hopping times of 500 ps. Above an exciton density of $\sim 6 \times 10^{17}\,cm^{-3}$, the short periodicity grating disappears on a time scale short compared to the 10 ps laser pulse, and the long periodicity grating no longer shows the $J = 1$ to $J = 2$ relaxation. The measured critical density is consistent with the $T = 0$ K Mott transition density given by $n^{1/3} a_B = 0.2$, where a_B is the Bohr radius of the bound exciton. We believe that the electron-hole plasma formed in the first few picoseconds is not in an equilibrium state and separates into low and high density phases on a time scale short compared to the ~ 20 ns fluorescence lifetime of the high density state [3]. Thus, we find that if one looks on a time scale short compared to some rough "condensation time", the transition from excitons (insulator) to plasma (metal) occurs over a very small change in exciton density.

1. N. F. Mott: *Metal Insulator Transitions* (Taylor and Francis, London 1974)
2. G. A. Thomas, T. M. Rice, J. C. Hensel, T. C. Phillips: *Electron Hole Drops*, Solid State Physics **32** (Academic Press, New York 1977)
3. J. E. Kardontchik, E. Cohen: Phys. Rev. B **19**, 3181 (1979)

Difference-Frequency Variation of the Free-Carrier-Induced Third Order Nonlinear Susceptibility in *n*-InSb

S. Y. Yuen and P. A. Wolff

Francis Bitter National Magnet Laboratory, Massachusetts Institute of Technology, Cambridge, MA 02139, USA

PACS: 42.65

The free-carrier-induced optical nonlinearity of semiconductors was first observed by Patel, Slusher, and Fleury (PSF) [1]. This effect was subsequently ascribed to band nonparabolicity by Wolff and Pearson (WP) [2]. To date, however, there has been no systematic investigation of the variation of the third order susceptibility $\chi^{(3)}$ with frequency difference, $\Delta\omega$, between the pump lasers. We have performed four-wave mixing experiments with Q-switched CO_2 lasers in n-InSb crystals with a variety of carrier concentrations. In all cases a dramatic increase in $\chi^{(3)}$ was observed as $\Delta\omega \to 0$.

Figure 1 shows the measured variation of the four-wave power versus difference frequency for an $n = 2\times10^{16}$ electrons/cm^3 sample with the polarization of the laser beams parallel to each other. The signal varies approximately as $(\Delta\omega)^{-2}$ for $30\,\mathrm{cm}^{-1} > \Delta\omega > 3\,\mathrm{cm}^{-1}$, then begins to saturate at smaller values of $\Delta\omega$. We find $\chi^{(3)} \simeq 2\times10^{-7}$ e.s.u. at the smallest difference frequency ($\Delta\omega = 1.4\,\mathrm{cm}^{-1}$) attainable with our CO_2 laser system. With laser beams polarized perpendicular to one another, the signals are greatly reduced in intensity, and the low frequency resonance is almost eliminated.

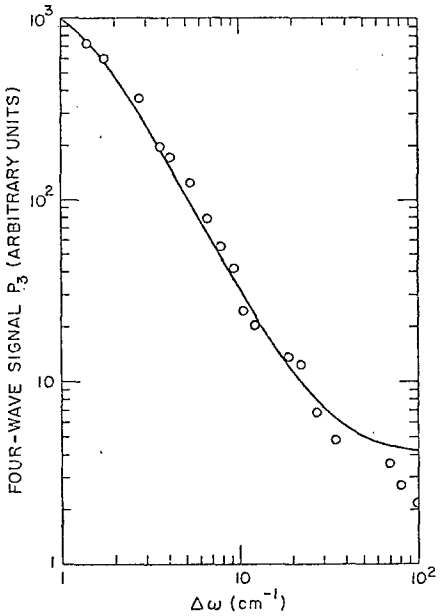

Fig. 1. Four wave signal versus frequency difference for $n = 2\times10^{16}\,\mathrm{cm}^{-3}$ InSb sample

This enhancement of $\chi^{(3)}$ as $\Delta\omega$ decreases is not predicted by WP, but can be explained by a model which requires that the velocity distribution of electrons in the crystal be modulated in two distinct ways by the optical fields. The distribution oscillates in velocity space, as discussed by WP. This process is non-dissipative in the limit $\omega\tau_m \to \infty$, τ_m being the momentum relaxation time when dissipation is taken into account. There is an irreversible flow of energy from the laser fields through the carriers into the lattice. This flow is also modulated at the frequency $\Delta\omega$, and thus causes a temperature fluctuation in the distribution. When the combined effects of these two perturbations are taken into account, the expression for the free-carrier-induced nonlinear susceptibility becomes:

$$\chi^{(3)}_{\mathrm{free}} = \frac{ne^4}{4m^{*2}E_g\omega_1^2\omega_2\omega_3}\left[1+\frac{2\tau_{th}-\tau_m}{\tau_m(1-i\Delta\omega\tau_{th})}\right]. \quad (1)$$

Here n is the free carrier density, ω_1, ω_2 are the laser frequencies $\omega_3 = 2\omega_1 - \omega_2$, and τ_{th} is the rate at which energy flows from the electron gas into the lattice. The first factor in (1) is the nonlinear susceptibility derived by WP. At large $\Delta\omega$, as in the case of PSF's experiments, $\chi^{(3)}_{\mathrm{free}}$ is almost independent of $\Delta\omega$. On the other hand, at low frequencies ($\Delta\omega\tau_{th} \ll 1$), the second term of (1) can exceed unit and cause an enhancement of $\chi^{(3)}_{\mathrm{free}}$. The value $\chi^{(3)} \simeq 2\times10^{-7}$ e.s.u. we measured is larger than any nonresonant susceptibility previously reported for $\Delta\omega \simeq 1\,\mathrm{cm}^{-1}$. Moreover, our model implies that $\chi^{(3)}_{\mathrm{free}}$ should increase in samples of lower mobility.

The low frequency enhancement of $\chi^{(3)}_{\mathrm{free}}$ has another important implication. Its saturation, as $\Delta\omega \to 0$, can be used to infer the energy relaxation time, τ_{th}. The solid curve in Fig. 1 was calculated from (1) with $\tau_{th} = 4\times10^{-12}$ s. This value is shorter than those measured with gentle excitation in n-InSb because in our work the electrons are highly excited by the power ful laser fields. Times in the picosecond range are not easy to measure directly. Thus, their measurement via the frequency dependence of the nonlinear susceptibility could prove a useful new technique in semiconductor research.

1. C.K.N.Patel, R.E.Slusher, P.A.Fleury: Phys. Rev. Lett. **17**, 1011 (1966)
2. P.A.Wolff, G.A.Pearson: Phys. Rev. Lett. **17**, 1015 (1966)

Novel Bifurcation Sequences in a Ring Bistable Cavity with an Input Gaussian Spatial Profile

J. V. Moloney, F. A. Hopf, and H. M. Gibbs

Optical Sciences Center, University of Arizona, Tucson, AZ 85721, USA

PACS: 42.65

Instabilities [1] associated with bistable branches of positive differential gain are investigated numerically for the case of a Gaussian input beam incident on a unidirectional ring cavity. The good-cavity limit permits an adiabatic elimination of the Bloch equations. The medium is characterized by a nonlinear complex absorption coefficient $\alpha_0(1+i\Delta)/(1+\Delta^2+I/I_s)$ where Δ is the detuning of the laser from resonance in units of $\gamma_\perp$, the dipole decay constant, and I_s is the saturation intensity. The Fresnel number F is $n_0a^2/\lambda L$ for a cylinder of HWHM radius a, length L, and refractive index n_0; F is 0.54 for the present transverse computation. The reflectivity of the ring cavity input and output mirrors is 0.9. The method of solution [2] employs a fast Fourier transform technique for medium and free-space propagation in the ring cavity; calculations here are confined to a single transverse Cartesian dimension.

Plane-wave and Gaussian on-axis bistable loops are directly compared in Fig. 1; the plane-wave unstable domain consists solely of a period 2 output (see figure caption for parameters). Details of the bifurcation sequences in each domain A and B of Fig. 1b are given by the on-axis dynamic outputs in Fig. 2A and B.

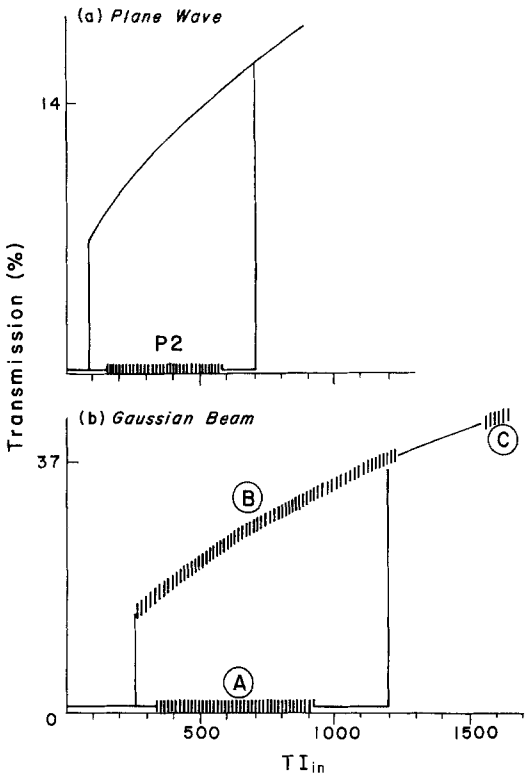

Fig. 1a and b. Bistable loops associated with a detuned ring cavity. Parameters used in the calculation are laser-cavity detuning $\beta_0 = 0.4$, $\Delta = 20$, $\alpha \equiv \alpha_0/(1+\Delta^2) = 1.66$, $T = 1 - R$, atomic medium fractional length is 0.15, free-space fractional length is 0.85. Input intensity I_{in} is in units of the saturation intensity I_s. (a) Plane wave, (b) Gaussian beam. On-axis transmitted intensity is shown

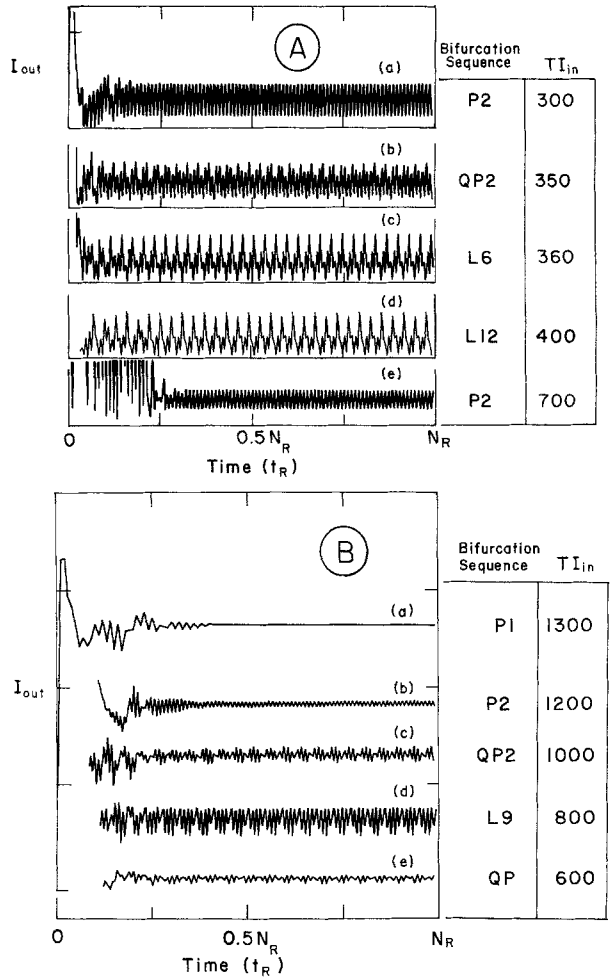

Fig. 2a–e. Dynamic outputs representing a sampling of the unstable domains A and B of Fig. 1b. The time axis is in units of t_R, the cavity round-trip time. A Dynamic outputs for region A. Number of cavity round trips $N_R = 200$. B Dynamic outputs for region B. (a) $N_R = 100$, (b) $N_R = 200$, (c) $N_R = 200$, (d) $N_R = 200$, (e) $N_R = 160$

Besides additional domains of instability for the Gaussian input, we observe bifurcation sequences which are in marked contrast to the plane-wave "period doubling" sequences [1]. The latter involve 2^N ($N \geqq 1$) sequences, possibly followed by chaos [1]. The dynamic outputs of Fig. 2A and B have symptotes which are characterized by an initial period 2 (P2) going through quasiperiodic (QP2) and frequency-locked (L6→L12, L9) behavior. The transverse output profiles exhibit rich and varied changes as the bifurcation sequence is mapped out; period 2 can involve oscillation between a Gaussian-like and doughnut-like transverse mode. Our results are consistent with recent experimentally observed bifurcations in hydrodynamics [3] and suggest that much can be learned about nonequilibrium phase transitions from a study of instabilities in optical bistability.

1. K.Ikeda: Opt. Commun. **30**, 257 (1979)
M.J.Feigenbaum: J. Stat. Phys. **19**, 25 (1978)
2. J.V.Moloney, H.M.Gibbs, M.R.Belic: Opt. Commun. (in press, 1982)
3. J.P.Gollub, S.V.Benson: J. Fluid Mech. **100**, 449 (1980)

Fluctuations in Optical Bistability: Experiments with Shot Noise

S. L. McCall
Bell Laboratories, Murray Hill, NJ 07974, USA
H. M. Gibbs, F. A. Hopf, D. L. Kaplan, and S. Ovadia
Optical Sciences Center, University of Arizona, Tucson, AZ 85721, USA

PACS: 42.65

Optical bistable devices [1] can be extrapolated to devices with a few atoms. Intrinsic fluctuations due to the finite number of atoms will then be a limitation. A hybrid bistable optical system has been modified to make shot noise dominant, so that fluctuation switching between states can be studied. Comparison is made with a direct simulation of the experiment and with master equation and Fokker-Planck descriptions. Under some circumstances the continuous Fokker-Planck description is inadequate, and a discrete Fokker-Planck-like or master equation approach must be used.

The semiclassical description of absorptive optical bistability for two-level atoms of peak absorption coefficient α_0 filling a cavity of length L and mirror transmissivity T leads to the requirement $\alpha_0 L/T > 8$ for bistability [2]. An optical cavity can have a waist about λ^2 in area. Choosing $T \simeq 0.05$, $\alpha_0 L \simeq 1$ is needed. Use a single atom whose absorption line is only broadened by lifetime effects. The absorption cross section is about λ^2, so $\alpha_0 L \simeq 1$ is achieved. Semiclassically, this single-atom device should be bistable. However, the semiclassical description is not valid because of quantum fluctuations which would cause the device to

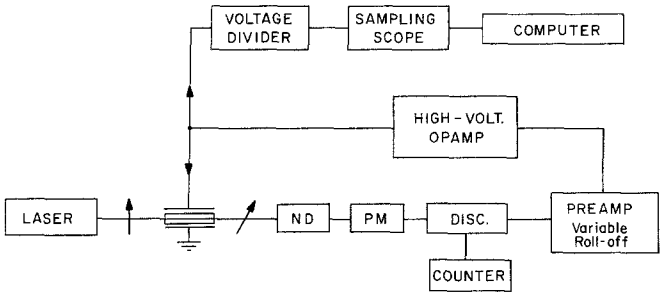

Fig. 1. Experimental apparatus

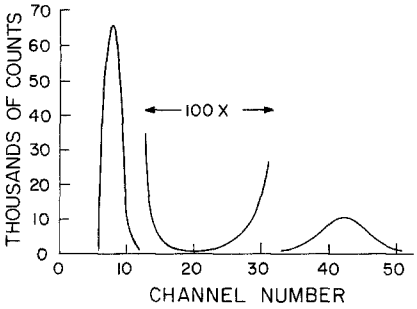

Fig. 2. Histogram of output voltage occurrences. Zero voltage is at about Channel 6, the lower state is about Channel 8, and the upper state about Channel 42

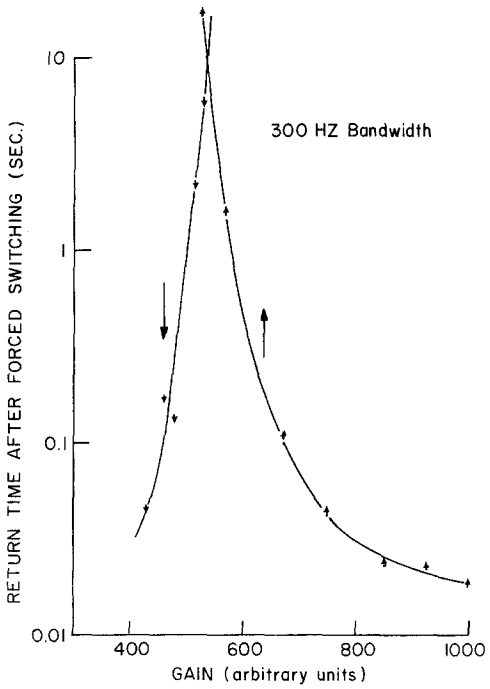

Fig. 3. Return time after forced switching to the lower state (↑ points) and to the upper state (↓ points) as a function of feedback gain setting. Switch-up and switch-down gains were ≃1000 and ≃400

switch states spontaneously. Since fundamental arguments do not rule out devices involving only a few absorbing centers and photons, the study of statistical limitations is especially relevant.

In the present experiment a hybrid device consisting of an electrooptic crystal between crossed polarizers is employed as shown in Fig. 1. The fluctuations are introduced and controlled by attenuating the transmitted light as it passes through the neutral density filter ND. The photomultiplier (PM) is operated in a single-photon-counting mode in which one standard pulse is generated for each PM pulse within the discriminator window. Note that this noise is smaller, in absolute value, when the system is in the lower state than when it is in the upper state. Many theories treat a state-independent noise term [1]. Data have been taken in two modes. In the first, the bistability operating point is selected so that switching back and forth occurs, and both dwell times and the distribution of voltages (Fig. 2) are recorded. In the other mode, the operating point can be anywhere within the bistable loop; the system is forced into one state by an external pulse and the time to return to the original state recorded (Fig. 3).

Computer simulations of the experiment show similar fluctuation switching. An analysis of the steady-state probability function leads to distributions similar to Fig. 2. Quantitative comparisons are underway.

1. For many papers on optical bistability and a few on fluctuations, see C.M.Bowden, M.Ciftan, H.R.Robl (eds.): *Optical Bistability* (Plenum Press, New York 1981)
2. A.Szöke, V.Daneu, J.Goldhar, N.A.Kurnit: Appl. Phys. Lett. **15**, 376 (1969)

The Dynamical Switching of a Bistable Optical Ring Cavity with Gaussian Input Beam Profile

J. V. Moloney and H. M. Gibbs

Optical Sciences Center, University of Arizona, Tucson, AZ 85721, USA

PACS: 42.65

Optical bistability switching transients have been calculated numerically including transverse effects and studied as a function of Fresnel number. The model employed is a Gaussian-transverse-profile input incident on a unidirectional ring cavity. Rapid medium response permits an adiabatic elimination of the Bloch equations. The transverse variations are assumed to occur in a single Cartesian coordinate permitting the use of fast Fourier transform propagation solutions. The medium is characterized by a nonlinear complex absorption coefficient $\alpha_0(1+i\Delta)/(1+\Delta^2+I/I_s)$ where Δ is the detuning of the laser from the resonance in resonance half-widths and I_s is the on-resonance saturation intensity. The Fresnel number is defined as $F=n_0a^2/\lambda L$ for a cylinder of HWHM radius a, length L, and refractive index n_0. The reflectivity of the ring cavity input and output mirrors is taken as 0.9.

For large Fresnel numbers switch-on occurs rapidly for radii out to the plane-wave switch-on intensity $I_\uparrow$; see Fig. 1a to e [1]. The diffraction of the discontinuity between the "on" inner spot and "off" outer part results in a very slow expansion of the "on" spot out to the plane-wave $I_\downarrow$. Self-focusing effects result in a highly modulated steady-state spatial output ring pattern (Fig. 2). For Fresnel numbers of order one or less, diffraction causes the beam to switch-on out to a large radius in a few cacity response times. The diffraction losses are so much greater for higher-order modes that only one mode characterizes the cavity and that mode is either "on" or "off". If diffraction is very strong the percentage transmission of the system is very small. However, a Fresnel number of order unity results in whole-beam switching, high

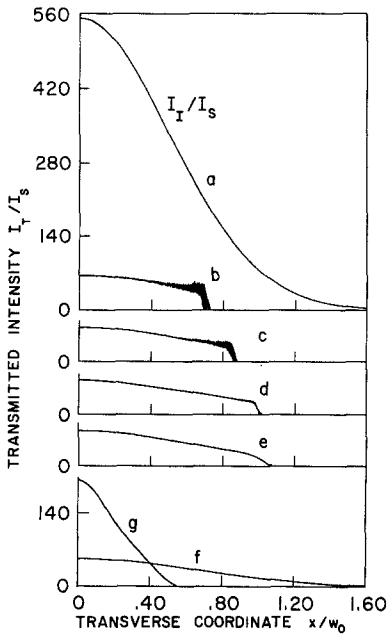

Fig. 1a–g. Switch-on in response to a step-function input. (a) Input profile I_I/I_s. (b)–(f) are for defocusing ($\Delta = -5$) and (g) is for focusing ($\Delta = +5$). (b)–(d): $F = 2200$ and round trips (b) 40–50, (c) 100–110, and (d) 230–240. (e) $F = 220$, round trips 98–100. (f) and (g): $F = 2.2$; round trips 40–50. The plane-wave $I_\uparrow$ is $200\,I_s$ and $I_\downarrow$ is $60\,I_s$, so the beamcenter intensity here is $\simeq 2.7\,I_\uparrow$. Not shown: I_T/I_s for $F = 22$ and $\Delta = -5$ falls off gradually, vanishing by $x/w_0 \simeq 1.2$; for $F = 0.22$ diffraction overcomes self-focusing and whole-beam switching occurs

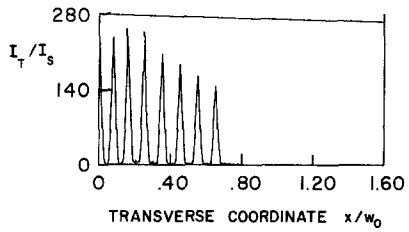

Fig. 2. Optical bistability switch-on in response to a step-function input for round trips 360 to 380 under high-Fresnel-number ($F = 870$), self-focusing ($\Delta = +5$) conditions. Steady-state may not have been reached yet

transmission, and fast response – characteristics desirable for practical devices.

The whole-beam switching found in the simulations for Fresnel numbers of order unity or less has been observed in an experiment using optical bistability in a GaAs etalon: $n_0 = 3.5$, $\lambda = 827$ nm, $a = 5\,\mu$m, $L = 4.5\,\mu$m, so $F \simeq 24$; the effective finesse was 8. Simultaneous switch-on and switch-off out to at least the radius for which the input drops to 5% was observed.

Acknowledgement. We are grateful for discussions with M. R. Belic, F. A. Hopf, and E. A. Watson.

1. N.N.Rosanov, V.E.Semenov: Opt. Commun. **38**, 435 (1981); Opt Spectrosc. (USSR) **48**, 108 (1980) report radially dependent switching for large F and use spatial filtering to avoid ringing. In contrast to our method, their model is a thin-sheet Kerr nonlinearity

Multistability in Coherently Driven Nonlinear Systems

D. F. Walls
Physics Department, University of Waikato, Hamilton, New Zealand

PACS: 42.65

The behaviour of coherently driven optical resonators filled with a nonlinear optical medium is reviewed. The phenomena of optical bistability is now well studied both experimentally and theoretically. We wish to investigate the phenomena which may arise when two or more cavity modes interact via the nonlinear medium. The cavity modes may have different frequencies, different polarizations or different directions of propagation. Two cavity modes may interact with a two photon absorber. If each cavity mode is driven with an equal amplitude the output may oscillate in three possible configurations. These are the symmetric configuration where each mode has the same amplitude or two nonsymmetric configurations where the modes have a different amplitude. Competition between the symmetric mode of oscillation and the two nonsymmetric modes results in regions of bi- and tristability. For low values of the driving field where the medium is unsaturated there is a pitchfork bifurcation and a change of stability from the symmetric to the nonsymmetric solutions. For higher values of the driving field the medium saturates and a third branch, the symmetric solution, becomes stable giving the possibility of optical tristability in this region. Two cavity modes interacting via a nonsaturable nonlinear medium, e.g. a Kerr type medium with nonlinear susceptibility $\chi^{(3)}$ exhibit a pitchfork bifurcation. However a three mode interaction via a nonlinear susceptibility $\chi^{(5)}$ exhibits an elliptic umbilic catastrophe to three possible nonsymmetric solutions. Three photon absorption exhibits a similar behaviour in the unsaturated region, however in the saturated region the symmetric solution also becomes stable giving four possible stable solutions. A fluctuation analysis leads to a steady state probability distribution from which the stability properties may be determined.

A three level atomic system interacting with two modes of the electromagnetic field is analysed. Different configurations of the three level atom are considered, i.e. the V, Λ and cascade configurations. For equal driving field amplitudes these systems show bifurcations from the symmetric to the nonsymmetric configuration. The limit in which the effective two level model is valid is explored.

These systems are a natural extension of the experiments performed on optical bistability. They provide an ideal opportunity to study mode competition in nonlinear optical systems.

1. D.F.Walls, C.V.Kunasz, P.D.Drummond, P.Zoller: Phys. Rev. **24** A, 627 (1981)